Arch Pharm Res Vol 33, No 10, 1641-1649, 2010
DOI 10.1007/s12272-010-1013-8

Archives of Pharmacal Research
www.springer.com/12272

Synthesis and Biological Evaluation of 3,6-diaryl-7*H*-thiazolo[3,2-*b*][1,2,4]triazin-7-one Derivatives as Acetylcholinesterase Inhibitors

Zhe Jin[1,2], Liu Yang[1,2], Si-Jie Liu[1,2], Jian Wang[1,2], Shuo Li[3], Huang-Quan Lin[3], David Chi Cheong Wan[3], and Chun Hu[1,2]

[1]Key Laboratory of Structure-Based Drug Design & Discovery, Ministry of Education, China, [2]School of Pharmaceutical Engineering, Shenyang Pharmaceutical University, Shenyang 110016, China, and [3]Department of Biochemistry, The Chinese University of Hong Kong, Hong Kong SAR, China

(Received April 21, 2010/Revised June 18, 2010/Accepted June 30, 2010)

Acetylcholinesterase (AChE) inhibitors played an important role in developing a cure for Alzheimer' s disease. In order to study on the influence of modifications at different groups and side chains on the AChE inhibitory ability and the active sites of 7*H*-thiazolo[3,2-*b*][1,2,4]triazin-7-one derivatives, fourteen 3,6-diaryl-7*H*-thiazolo[3,2-*b*][1,2,4]triazin-7-one derivatives were designed and synthesized. The study of AChE inhibitory activity was carried out using the Ellman colorimetric assay with huperzine-A as the positive control drug. Most of the target compounds exhibited more than 50% inhibition at 10 μM. Some target compounds showed strong inhibition against AChE. The molecular fields analysis and preliminary structure-activity relationships are discussed.

Key words: Acetylcholinesterase, Inhibitor, Heterocycle, Thiazole, 1,2,4-Triazine, Molecular docking, Molecular fields analysis

INTRODUCTION

Alzheimer's disease (AD) is the most common age-related neurodegenerative disorder (LaFerla et al., 2007). In the United States, an estimated 4.5 million individuals are currently suffering from AD (Hebert et al., 2003). According to a survey released by the Shanghai Mental Health Centre in the 1990s, approximately 4.69% people in Shanghai China suffered from AD (Wang et al., 2002). As a result, AD treatment and care constitutes a major social and health problem (Ceballos and Guzman, 2005).

To date, acetylcholinesterase (AChE) inhibitors are the main type of drugs used to treat AD. Current medications that have received FDA approval for the treatment of AD include AChE inhibitors, such as tacrine, donepezil, rivastigmine, galanthamine, and an NMDA receptor antagonist, memantine.

Correspondence to: Chun Hu, Department of Organic Chemistry, Shenyang Pharmaceutical University, Shenyang 110016, China
Fax: 86-24-23986050
E-mail: chunhu@syphu.edu.cn

In recent years, a series of crystal structures of the *Torpedo californica* AChE (*Tc*AChE) and human AChE (*h*AChE) have been reported. In *Tc*AChE, the structure indicated that there is a deep, narrow gorge approximately 200 nm long on the surface of the enzyme, called the catalytic active site (CAS), which was assigned to the Ser-His-Glu catalytic triad (Ser200-His440-Glu327). In the middle of the gorge, there are 5 amino acid residues, including Trp84, Tyr130, Glu199, Phe330, and Tyr442, which comprise the anionic binding site. At the entrance of the aromatic gorge, there is a peripheral anionic site (PAS), including Tyr70, Asp72, Tyr121, Glu278, Trp279, and Tyr334 residues (Sussman et al., 1991; Khalid et al., 2004).

Previously, the interaction between 4 inhibitors, tacrine (Davis and Powchik, 1995; Shao and Li, 2004), donepezil (Kryger et al., 1999; Tsuno, 2009), rivastigmine (Polinsky, 1998; Grossberg, 2005), huperzine A (Raves et al., 1997; Bai et al., 2000), and AChE, have been investigated by flexible docking and X-ray diffraction crystal structure of the AChE inhibitor-AChE complex. These results showed that some AChE inhibitors, such as donepezil, interact with the PAS and

the anionic binding site of AChE, while other inhibitors, such as rivastigmine, interact with the CAS of AChE. Recent studies have suggested that dual-binding inhibitors not only increase the inhibitory activity and selectivity of AChE but also prevent the aggregation of toxic β-amyloid (Aβ) (Inestrosa et al., 1996; Reyes et al., 1997). Hence, dual-binding AChE inhibitors, which interact with the PAS and the CAS of AChE, are hot topics in research on AChE inhibitors.

Our previous work has shown 5*H*-thiazolo[3,2-*a*]pyrimidine derivatives exhibited AChE inhibitory activity, and the molecular docking exhibited the compounds interacted with the PAS of AChE (Zhi et al., 2008). 6-Arylmethyl-7*H*-thiazolo[3,2-*b*][1,2,4]triazin-7-one derivatives also exhibited AChE inhibitory activity, and the molecular docking exhibited the compounds interacted with the PAS and the CAS of AChE (Liu et al., 2009).

In order to study the the structure-AChE inhibitory activity relationships and the active sites of 7*H*-thiazolo[3,2-*b*][1,2,4]triazin-7-one derivatives, a new series of 3,6-diaryl-7*H*-thiazolo[3,2-*b*][1,2,4]triazin-7-one derivatives were designed and synthesized, and their inhibitory activity was determined.

MATERIALS AND METHODS

Molecular docking

The crystal structure of the *h*AChE (1B41/fasciculin-2) complex was selected from the Protein Data Bank. The inhibitor structure and water molecules were deleted from the complex, the missing residues were built in, and the polar hydrogen atoms were added to the amino acid residues. Molecular docking was carried out using the Molegro Virtual Docker (MVD) (Thomsen and Christensen, 2006). The docking algorithm was set at 1,500 maximum iterations with a simplex evolution population size of 50 and a minimum of 10 runs. Schematic diagrams of the interactions between 1B41 and the small molecules were analyzed using MVD.

Chemistry

All reagents and solvents were purchased from common commercial suppliers and were used without further purification. Melting points were determined on a Koffler hot-plate apparatus and were uncorrected. The C, H, and N element analyses were performed on a Thermo Flash EA1112 elemental analyzer. Mass spectra (MS) were obtained using an electronic impact (EI) ion source at 70 eV in an Agilent spectrometer (with direct insertion probe) or with an electrospray (ESI) ion source in a Waters spectrometer at 3.5 kV spray voltage, acetonitrile was used as the solvent. ^{1}H-NMR spectra were obtained in DMSO-d_6 or $CDCl_3$ on a Bruker spectrometer operating at 300 MHz or 600 MHz. The IR spectra were determined using a Bruker AFS55 spectrometer.

Synthesis of 2-aryl-2-oxoacetic acids (2)

A mixture of styrene derivatives (**1**) (0.06 mol), NaOH (0.06 mol), and $KMnO_4$ (0.09 mol) were dissolved in H_2O (500 mL) in a 1000 mL round bottom flask, heated to 50°C, and stirred for 20 min. Ethanol (20 mL) was then dropped slowly into the flask and stirred for 15 min. The mixture was filtered, washed with hot water, concentrated, acidified with concentrated HCl, and extracted with ethyl acetate (25 mL × 4). The organic layer was dried and distilled to give 2-aryl-2-oxoacetic acid.

2-(4-Chlorophenyl)-2-oxoacetic acid (2a)

White solid, 60% yield. Only one spot on thin layer chromatography (TLC), spreading solvents were acetate/n-hexane (V/V = 2/1), R_f = 0.32.

2-(4-Bromophenyl)-2-oxoacetic acid (2b)

White solid, 76% yield. Only one spot on TLC, spreading solvents were acetate/n-hexane (V/V = 2/1), R_f = 0.30.

Synthesis of 6-aryl-3-thioxo-3,4-dihydro-1,2,4-triazin-5(2*H*)-ones (3)

A mixture of **2** 0.20 mol, thiosemicarbazide (0.25 mol), ethanol (20 mL), and concentrated NaOH in aqueous solution (15 mL) was refluxed for 7 h, cooled to room temperature, and adjusted to pH 2 with HCl. The solid was collected to give 6-(4-halophenyl)-3-thioxo-3,4-dihydro-1,2,4-triazin-5(2*H*)-one.

6-(4-Chlorophenyl)-3-thioxo-3,4-dihydro-1,2,4-triazin-5(2*H*)-one (3a)

White powder, 72% yield; mp: 279-282°C.

6-(4-Bromophenyl)-3-thioxo-3,4-dihydro-1,2,4-triazin-5(2*H*)-one (3b)

Yellowish powder, 67% yield; mp: 272-275°C.

Synthesis of 3, 6-diaryl-7*H*-thiazolo[3,2-*b*][1,2,4]triazin-7-ones (4)

A mixture of 6-aryl-3-thioxo-3,4-dihydro-1,2,4-triazin-5(2*H*)-one (10 mmol), substituted phenacyl chloride (10 mmol), and AcOH (20 mL) was heated under reflux for 12 h. The solution was then cooled to room temperature and filtered. The solid was collected and recrystallized from absolute ethanol.

3-(4-Methylphenyl)-6-phenyl-7*H*-thiazolo[3,2-*b*][1,2,4]triazin-7-one (4a)
Yellowish powder, 66% yield; mp: 221-223°C; ESI-MS *m/z* (relative intensity): 320.0 ($[M+H]^+$, 17), 341.9 ($[M+Na]^+$, 62), 661.0 ($[2M+Na]^+$, 100); ^{1}H-NMR (300 MHz, $CDCl_3$): δ 8.23 (2H, dd, *J* = 6.5 Hz), 7.61 (2H, d, *J* = 8.13 Hz), 7.48 (2H, m), 7.46 (2H, d, *J* = 7.7 Hz), 7.34 (2H, d, *J* = 7.8 Hz), 6.84 (1H, s), 2.46 (3H, s); IR (KBr, cm^{-1}): υ 3069, 1638, 1538, 1468, 1384, 1350, 542; Anal. calcd. for $C_{18}H_{13}ON_3S$ (%): C, 67.69; H, 4.10; N, 13.16; S, 10.04; Found (%): C, 67.63; H, 4.05; N, 13.13.

3-(4-Chlorophenyl)-6-phenyl-7*H*-thiazolo[3,2-*b*][1,2,4]triazin-7-one (4b)
Yellowish powder, 59% yield; mp: 269-271°C; ESI-MS *m/z* (relative intensity): 339.9 ($[M+H]^+$, 13), 361.9 ($[M+Na]^+$, 100), 700.8 ($[2M+Na]^+$, 16); ^{1}H-NMR (300 MHz, $CDCl_3$): δ 8.20 (2H, d, *J* = 7.8 Hz), 7.66 (2H, d, *J* = 8.4 Hz), 7.53 (2H, d, *J* = 8.4 Hz), 7.47 (2H, d, *J* = 7.2 Hz), 6.90 (1H, s); IR (KBr, cm^{-1}): υ 3067, 1642, 1537, 1471, 1383, 1353, 547; Anal. calcd. for $C_{17}H_{10}ON_3SCl$ (%): C, 60.09; H, 2.97; N, 12.37; Found (%): C, 60.03; H, 2.94; N, 12.33.

6-Phenyl-3-(4-tert-butylphenyl)-7*H*-thiazolo[3,2-*b*][1,2,4]triazin-7-one (4c)
Yellowish powder, 62% yield; mp: 216-217°C; ESI-MS *m/z* (relative intensity): 400.0 ($[M+K]^+$, 69); ^{1}H-NMR (600 MHz, $CDCl_3$): δ 8.21 (2H, m), 7.66 (2H, d, *J* = 7.8 Hz), 7.55 (2H, d, *J* = 8.4 Hz), 7.49 (1H, d, *J* = 7.8 Hz), 7.45 (2H, m), 6.84 (1H, s), 1.40 (9H, s); IR (KBr, cm^{-1}): υ 3087, 2961, 1637, 1543, 1469, 1384, 546; Anal. calcd. for $C_{21}H_{19}ON_3S$ (%): C, 69.78; H, 5.30; N, 11.63; Found (%): C, 69.71; H, 5.27; N, 11.58.

3-(4-Methoxy-3-methylphenyl)-6-phenyl-7*H*-thiazolo[3,2-*b*][1,2,4]triazin-7-one (4d)
Yellowish powder, 61% yield; mp: 234-236°C; ESI-MS *m/z* (relative intensity): 349.9 ($[M+H]^+$, 14), 372.0 ($[M+Na]^+$, 100), 721.0 ($[2M+Na]^+$, 22); ^{1}H-NMR (600 MHz, $CDCl_3$): δ 8.22 (2H, m), 7.54 (1H, dd, J_1 = 8.4 Hz, J_2 = 2.4 Hz), 7.48 (2H, d, *J* = 7.2 Hz), 7.44 (2H, dd, J_1 = 7.8 Hz, J_2 = 1.2 Hz), 6.95 (1H, d, J_1 = J_2 = 8.4 Hz), 6.76 (1H, s), 3.91 (3H, s), 2.29 (3H, s); IR (KBr, cm^{-1}): υ 3135, 2919, 1684, 1567, 1469, 1385, 1329, 562; Anal. calcd. for $C_{19}H_{15}O_2N_3S$ (%): C, 65.31; H, 4.33; N, 12.03; Found (%): C, 65.26; H, 4.28; N, 11.97.

3-(4-Hydroxy-3-methylphenyl)-6-phenyl-7*H*-thiazolo[3,2-*b*][1,2,4]triazin-7-one (4e)
Yellowish powder, 60% yield; mp: 201-203°C; ESI-MS *m/z* (relative intensity): 336.1 ($[M+H]^+$, 57), 358.2 ($[M+Na]^+$, 100), 693.4 ($[2M+Na]^+$, 25); ^{1}H-NMR (600 MHz, DMSO-d_6): δ 9.88 (1H, s), 7.98 (2H, d, *J* = 9.0 Hz), 7.50 (1H, d, *J* = 7.8 Hz), 7.48 (2H, d, *J* = 7.8 Hz), 7.46 (1H, s), 6.91 (1H, d, *J* = 7.8 Hz), 2.50 (3H, s); IR (KBr, cm^{-1}): υ 3048, 1774, 1635, 1545, 1466, 1282, 689, 527; Anal. calcd. for $C_{18}H_{13}O_2N_3S$ (%): C, 64.46; H, 3.91; N, 12.53; Found (%): C, 64.38; H, 3.86; N, 12.48.

6-(4-Chlorophenyl)-3-phenyl-7*H*-thiazolo[3,2-*b*][1,2,4]triazin-7-one (4f)
White powder, 39% yield; mp: 283-285°C; ESI-MS *m/z* (relative intensity): 339.9 ($[M+H]^+$, 100), 341.9 ($[M+2+H]^+$, 34), 361.9 ($[M+Na]^+$, 48), 363.9 ($[M+2+Na]^+$, 18); ^{1}H-NMR (300 MHz, DMSO-d_6): δ 8.02 (2H, d, *J* = 8.4 Hz), 7.76 (5H, m), 7.71 (2H, d, *J* = 8.4 Hz), 7.66 (1H, s); IR (KBr, cm^{-1}): υ 3063, 1632, 1541, 1469, 1384, 1353, 840, 759; Anal. calcd. for $C_{17}H_{10}ON_3SCl$ (%): C, 60.09; H, 2.97; N, 12.37; Found (%): C, 60.03; H, 2.94; N, 12.33.

3-(4-Chlorophenyl)-6-(4-bromophenyl)-7*H*-thiazolo[3,2-*b*][1,2,4]triazin-7-one (4g)
Yellow needle crystal, 12% yield; mp: 314-316°C; ESI-MS *m/z* (relative intensity): 417.7 ($[M+H]^+$, 29), 419.8 ($[M+2+H]^+$, 40), 421.8 ($[M+4+H]^+$, 13); 439.7 ($[M+Na]^+$, 63), 441.7 ($[M+2+Na]^+$, 100); 455.7 ($[M+K]^+$, 21), 457.7 ($[M+2+K]^+$, 31), 459.7 ($[M+4+K]^+$, 16); ^{1}H-NMR (300 MHz, DMSO-d_6): δ 8.02 (2H, d), 7.92 (2H, d), 7.74 (4H, m), 7.53 (1H, s); IR (KBr, cm^{-1}): υ 3443, 3079, 1642, 1535, 1466, 1384, 1279, 835, 520; Anal. calcd. for $C_{17}H_9ON_3SClBr$ (%): C, 48.77; H, 2.17; N, 10.04; Found (%): C, 48.70; H, 2.14; N, 9.99.

6-(4-Bromophenyl)-3-(4-methylphenyl)-7*H*-thiazolo[3,2-*b*][1,2,4]triazin-7-one (4h)
Yellow powder, 31% yield; mp: 283-286°C; ESI-MS *m/z* (relative intensity): 398.0 ($[M+H]^+$, 62), 400.0 ($[M+2+H]^+$, 58), 420.0 ($[M+Na]^+$, 79), 422.0 ($[M+2+Na]^+$, 100), 436.0 ($[M+K]^+$, 60), 438.0 ($[M+2+K]^+$, 82); ^{1}H-NMR (300 MHz, DMSO-d_6): δ 8.02 (2H, d, *J* = 8.4 Hz), 7.87 (2H, d, *J* = 8.4 Hz), 7.72 (2H, d, *J* = 8.4 Hz), 7.53 (1H, s), 7.36 (2H, d, *J* = 8.4 Hz), 2.39 (3H, s); IR (KBr, cm^{-1}): υ 3425, 3066, 1635, 1539, 1466, 837, 815, 550, 524; Anal. calcd. for $C_{18}H_{12}ON_3SBr$ (%): C, 54.28; H, 3.04; N, 10.55; Found (%): C, 54.21; H, 3.00; N, 10.50.

6-(4-Chlorophenyl)-3-(4-methoxyphenyl)-7*H*-thiazolo[3,2-*b*][1,2,4]triazin-7-one (4i)
Yellow powder, 36% yield; mp: 291-293°C; ESI-MS *m/z* (relative intensity): 370.1 ($[M+H]^+$, 67), 392.1 ($[M+Na]^+$, 100), 394.0 ($[M+2+Na]^+$, 39), 408.0 ($[M+K]^+$, 55), 410.0 ($[M+2+K]^+$, 27); ^{1}H-NMR (300 MHz, DMSO-d_6): δ 8.10 (2H, d, *J* = 8.7 Hz), 7.73 (2H, d, *J* = 8.7 Hz), 7.57 (2H, d, *J* = 8.7 Hz), 7.48 (1H, s), 7.11 (2H, d, *J* =

8.7 Hz), 3.36 (3H, s); IR (KBr, cm^{-1}): υ 3443, 3067, 1645, 1538, 1466, 1384, 1254, 837, 524; Anal. calcd. for $C_{18}H_{12}O_2N_3SCl$ (%): C, 58.46; H, 3.27; N, 11.36; Found (%): C, 58.41; H, 3.24; N, 11.31.

3-(4-Hydroxyphenyl)-6-phenyl-7*H*-thiazolo[3,2-*b*][1,2,4]triazin-7-one (4j)

Yellowish powder, 60% yield; mp: 171-172°C; ESI-MS *m/z* (relative intensity): 343.9 ($[M+Na]^+$, 100), 664.8 ($[2M+Na]^+$, 14); ^{1}H-NMR (300 MHz, DMSO-d_6): δ 9.95 (2H, d, J = 8.4 Hz), 8.06 (2H, dd, J_1 = 7.2 Hz, J_2 = 1.5 Hz), 7.61 (2H, d, J = 8.7 Hz), 7.49 (3H, m), 7.39 (1H, s), 6.92 (1H, s), 6.89 (1H, s); IR (KBr, cm^{-1}): υ 3118, 1720, 1610, 1507, 1471, 1384, 1325, 548; Anal. calcd. for $C_{17}H_{11}O_2N_3S$ (%): C, 63.54; H, 3.45; N, 13.08; Found (%): C, 63.49; H, 3.40; N, 13.04.

6-(4-Bromophenyl)-3-(4-methoxyphenyl)-7*H*-thiazolo[3,2-*b*][1,2,4]triazin-7-one (4k)

Yellow powder, 26% yield; mp: 289-291°C; ESI-MS *m/z* (relative intensity): 414.0 ($[M+H]^+$, 85), 416.0 ($[M+2+H]^+$, 77), 436.0 ($[M+Na]^+$, 100), 438.0 ($[M+2+Na]^+$, 81), 452.0 ($[M+K]^+$, 40), 454.0 ($[M+2+K]^+$, 47); ^{1}H-NMR (300 MHz, DMSO-d_6): δ 8.02 (2H, d, J = 8.7 Hz), 7.72 (4H, m), 7.48 (1H, s), 7.11 (2H, d, J = 8.7 Hz), 3.84 (3H, s); IR (KBr, cm^{-1}): υ 3423, 3068, 1643, 1586, 1538, 1465, 1384, 1278, 1255, 1179, 1078, 1010, 835, 553, 521; Anal. calcd. for $C_{18}H_{12}O_2N_3SBr$ (%): C, 52.19; H, 2.92; N, 10.14; Found (%): C, 52.10; H, 2.88; N, 10.09.

Synthesis of 3,6-diaryl-7*H*-thiazolo[3,2-*b*][1,2,4]triazin-7-ones (5)

A mixture of 3-(4-hydroxyphenyl)-6-aryl-7*H*-thiazolo [3,2-b][1,2,4]triazin-7-one (10 mmol), 2-chloro-*N*,*N*- diethylacetamide or 2-chloro-1-(piperidin-1-yl)ethanone or *N*-benzyl-2-chroloacetamide (10 mmol), potassium carbonate (50 mmol), potassium iodide (1 mmol), and acetone (25 mL) was heated under reflux for 24 h. Then the mixture was poured into H_2O (100 mL) and stirred for 12 h. The solid was collected and recrystallized from absolute ethanol.

3-[4-(2-Dimethylamino-2-oxoethoxy)phenyl]-6-phenyl-7*H*-thiazolo[3,2-*b*][1,2,4]triazin-7-one (5a)

Yellowish powder, 70% yield; mp: 231-233°C; ESI-MS *m/z* (relative intensity): 407.1 ($[M+H]^+$, 16), 429.2 ($[M+Na]^+$, 100), 835.3 ($[2M+Na]^+$, 15); ^{1}H-NMR (600 MHz, DMSO-d_6): δ 8.04 (2H, d, J = 7.8 Hz), 7.71 (2H, m), 7.53 (1H, d, J = 7.2 Hz), 7.49 (2H, d, J = 7.8 Hz), 7.47 (1H, s), 7.08 (2H, m), 4.91 (2H, s), 3.00 (3H, s), 2.85 (3H, s); IR (KBr, cm^{-1}): υ 3135, 2926, 1667, 1592, 1471, 1386, 1355, 1317, 557; Anal. calcd. for $C_{21}H_{18}O_3N_4S$ (%): C, 62.06; H, 4.46; N, 13.78; Found (%): C, 61.99; H, 4.41; N, 13.73.

3-{4-[2-Oxo-2-(4-morpholinyl)ethoxy]phenyl}-6-phenyl-7*H*-thiazolo[3,2-*b*][1,2,4]triazin-7-one (5b)

Yellowish powder, 60% yield; mp: 129-130°C; ESI-MS *m/z* (relative intensity): 449.3 ($[M+H]^+$, 22), 471.2 ($[M+Na]^+$, 100); ^{1}H-NMR (600 MHz, DMSO-d_6): δ 8.03 (2H, d, J = 7.2 Hz), 7.71 (2H, d, J = 9.0 Hz), 7.51 (1H, d, J = 7.8 Hz), 7.48 (2H, d, J = 7.8 Hz), 7.47 (1H, s), 7.09 (2H, d, J = 8.4 Hz), 4.94 (2H, s), 3.62 (2H, t), 3.57 (2H, t), 3.45 (4H, d, J = 13.2 Hz); IR (KBr, cm^{-1}): υ 3114, 2971, 1635, 1545, 1469, 1384, 1351, 551; Anal. calcd. for $C_{23}H_{20}O_4N_4S$ (%): C, 61.60; H, 4.49; N, 12.49; Found (%): C, 61.52; H, 4.45; N, 12.45.

3-{4-[2-(4-Piperidyl)ethoxy]phenyl}-6-phenyl-7*H*-thiazolo[3,2-*b*][1,2,4]triazin-7-one (5c)

Yellowish powder, 65% yield; mp: 151-153°C; ESI-MS *m/z* (relative intensity): 433.3 ($[M+H]^+$, 100); ^{1}H-NMR (600 MHz, DMSO-d_6): δ 8.05 (2H, d, J = 6.6 Hz), 7.71 (2H, d, J = 9.0 Hz), 7.51 (1H, d, J = 7.2 Hz), 7.48 (2H, d, J = 7.8 Hz), 7.46 (1H, s), 7.12 (2H, d, J = 9.0 Hz), 4.14 (2H, t, J_1 = J_2 = 6.0 Hz), 2.68 (2H, m), 2.48 (4H, m), 1.50 (4H, m), 1.38 (2H, s); IR (KBr, cm^{-1}): υ 3070, 2931, 1636, 1544, 1473, 1384, 1351, 549; Anal. calcd. for $C_{24}H_{24}O_2N_4S$ (%): C, 66.64; H, 5.59; N, 12.95; Found (%): C, 66.57; H, 5.57; N, 12.91.

Inhibition of AChE

The compounds dissolved in DMSO were tested for AChE inhibitory activity by the Ellman assay (Elsinghorst et al., 2006). The Ellman assay was performed in 96 well plates as follows: the compound in assay buffer (100 mM sodium phosphate buffer, pH 7.4) was mixed with 0.1 unit of *h*AChE (Sigma, C-1682). After a 15 min pre-incubation, equal amounts of 12.5 mM of acetylthiocholine iodide (ATCI) (Sigma, A-5751) and 10 mM 5'5-dithio-bis-(2-nitrobenzoate) DTNB (Sigma, D-8130) were added, and then 100 μL of the mixture was added to individual wells. After a 20 min incubation with the substrate, the optical densities were measured in a 96-well plate reader at 415 nm. The optical density was inversely proportional to the inhibitory activity. Percentage inhibitions were calculated as compared to control. Data analysis was performed with Sigma Plot 2001 software. Inhibitory effects were expressed as the percentage of inhibition.

RESULTS AND DISCUSSION

Docking studies

Comparison of the three-dimensional structures of

*Tc*AChE (1EVE) and *h*AChE (1B41) revealed a high degree of similarity, especially with regard to the active sites. The most significant difference between the active sites of *Tc*AChE and *h*AChE is that the Phe330 of *Tc*AChE was replaced with a Tyr337 of *h*AChE. Another difference is that the sequence number of some protein residues; for example, Ser200 of *Tc*AChE was replaced by Ser203 of *h*AChE (Sussman et al., 1991; Kryger et al., 1999) (Table I).

The action sites of the various inhibitors and AChE are also different (Table II). Tacrine was shown to interacts with the CAS and the PAS of AChE (Shao and Li, 2004), donepezil with the PAS and the anionic binding site of AChE (Kryger et al., 1999), rivastigmine with the CAS of AChE (Polinsky, 1998), and huperzine A with the CAS and the anionic binding site of AChE (Raves et al., 1997).

All of the target compounds were overlapped in the active sites of *h*AChE (Fig. 1). The residues were color coded as follows: the amino acid residues of CAS are shown in gray, the residues of anionic binding site are shown in green, and the residues of PAS are shown in yellow. There was a high degree of overlap between all of the target compounds, especially the scaffold moiety, the active sites of the target compounds were similar. The long side chains of the compounds **5a**-**5c** were also able to interact with *h*AChE and extraordinary active sites.

According to the predicted docking interactions between 3-(4-hydroxy-3-methylphenyl)-6-phenyl-7*H*-thiazolo[3,2-*b*][1,2,4]triazin-7-one (**4e**) and *h*AChE, hydrogen bonds (represented as green dotted lines, Fig. 2) occur between the carbonyl group at the C7 position, the C8 position of the parent nucleus of com-

Table I. Differences in the protein residues of *Tc*AChE and *h*AChE

Active Site	*Tc*AChE	*h*AChE	Active Site	*Tc*AChE	*h*AChE
Catalysis active site (CAS)	Ser200	Ser203	Peripheral anionic site (PAS)	Tyr70	Tyr72
	Glu327	Glu334		Asp72	Asp74
	His440	His447		Tyr121	Tyr124
Anionic binding site	Trp84	Trp86		Glu278	Glu285
	Tyrl30	Tyr133		Trp279	Trp286
	Glu199	Glu202		Tyr334	Tyr341
	Phe330	**Tyr337**			
	Tyr442	Tyr449			

Table II. Different inhibitors interacted with different active sides of the AChE

AChE Inhibitor	Protein Residues	Active Sites	AChE Inhibitor	Protein Residues	Active Sites
Tacrine	His440	CAS	Rivastigmine	Ser200	CAS
	Asp72	PAS	Huperzine A	His440	CAS
Donepezil	Trp279	PAS		Trp84, Tyr130	Anionic binding site
	Trp84, Phe330	Anionic binding site		Glu199, Phe330	

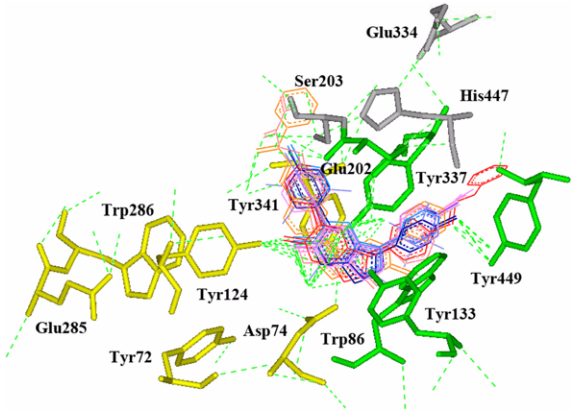

Fig. 1. Docking model of the target compounds superimposed in the active sites of *h*AChE

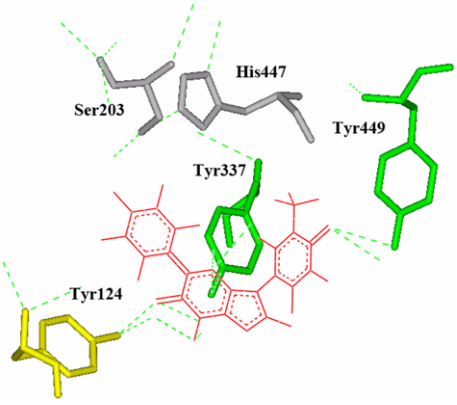

Fig. 2. Docking model of compound **4e** in the active sites of *h*AChE

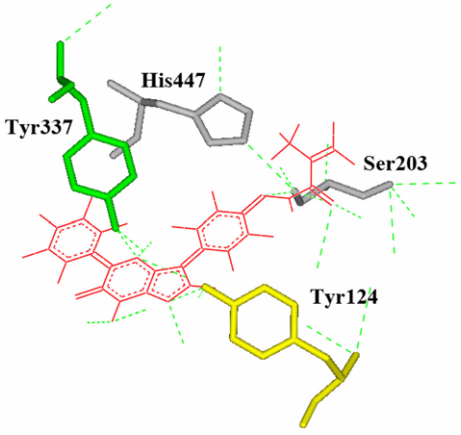

Fig. 3. Docking model of compound **5a** in the active sites of *h*AChE

pound **4e** and the Tyr124 of *h*AChE, between the N5 position of the parent nucleus and the Tyr337 residue, and between the hydroxyl group at the aromatic ring at the C3 position of the parent nucleus and Tyr 449. The protein residue Tyr124 was shown to be located in the peripheral anionic site (PAS) and Tyr337 and Tyr449 in the anionic binding site (Table I). Compound **4e** is thought to interact with the PAS and the anionic binding site of *h*AChE.

Similarly, there are predicted hydrogen bonds between the parent nucleus of 3-[4-(2-dimethylamino-2-oxoethoxy)phenyl]-6-phenyl-7*H*-thiazolo[3,2-*b*][1,2,4] triazin-7-one (**5a**) and Tyr124, Tyr337 of *h*AChE (Fig. 3) and the parent side chains of compound **5a** and Ser203 of *h*AChE. It was also determined that the protein residue Ser203 is located in the catalysis active site (CAS), Tyr124 is located in the PAS, and Tyr337 is located in the anionic binding site. Hence the target compound **5a** can interact with the CAS, the PAS, and the anionic binding site of *h*AChE.

Chemistry

The target compounds **4a-k** were obtained in satisfactory yields, and the synthetic pathways are described in Scheme 1.

The target compounds 3-substituted aryl 7*H*-thiazolo[3,2-*b*]-1,2,4-triazin-7-one derivatives **5a-c** were obtained with the classical Williamson reaction shown in Scheme 2.

The general procedure, described below, was developed for the generation of synthetic target compounds. The styrene derivatives (**1**) were synthesized with yields from 60 to 73% in accordance with the literature (Marvel and Schertz, 1943). Compound **1** reacted with the $KMnO_4$ alkaline aqueous solution to produce keto acids **2**. Compound **3** was prepared by a reaction of compound **2** with thiosemicarbazide in a sodium hydroxide aqueous solution. The target compounds **4a-k** were obtained by a reaction of compound **3** with substituted phenacyl chlorides in acetic acid. The target compounds **5a-c** were prepared with the Williamson reaction shown in Scheme 2 (Ahmad et al., 1987; Liu et al., 1992; Ramadan et al., 2005).

The chemical structures of all target compounds synthesized were fully characterized by mass spectra (MS), element analysis, ^{1}HNMR, and infrared spectra data.

Inhibition of AChE

The biological activity of *h*AChE (0.5 units) was tested against the target compounds. Each compound was tested three times (n = 3), while shaking for 20 min. Inhibition of *h*AChE activity by the positive control, huperzine-A, (10 μM; n = 3) was 100%.

The compounds **4e** and **4j**, which have a hydroxyl group, exhibited a more potent inhibitory effect than **4a-d** because the hydroxyl group was able to form a hydrogen bond with Tyr449 of the AChE receptor

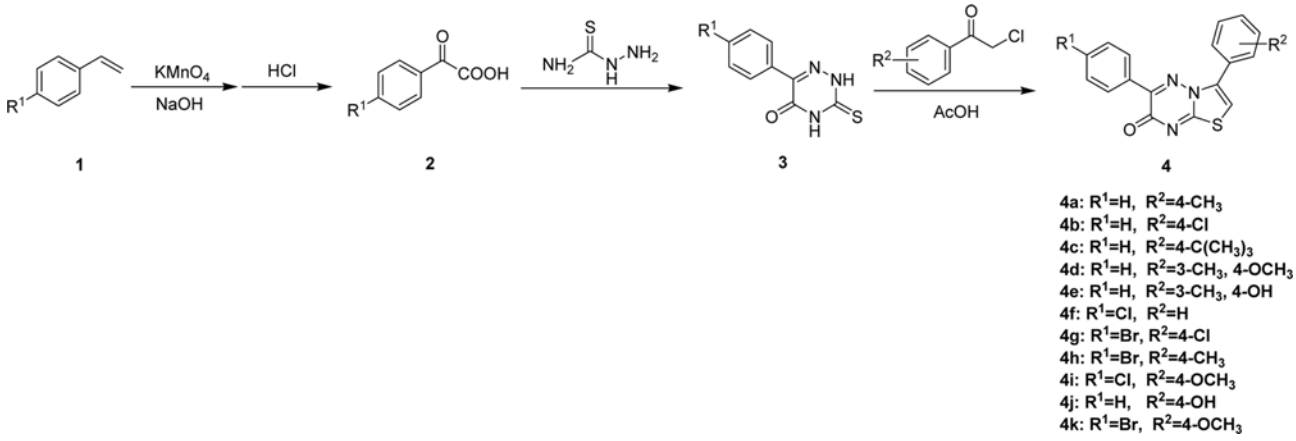

Scheme 1. The synthetic route of 7*H*-thiazolo[3,2-*b*]-1,2,4-triazin-7-one derivatives

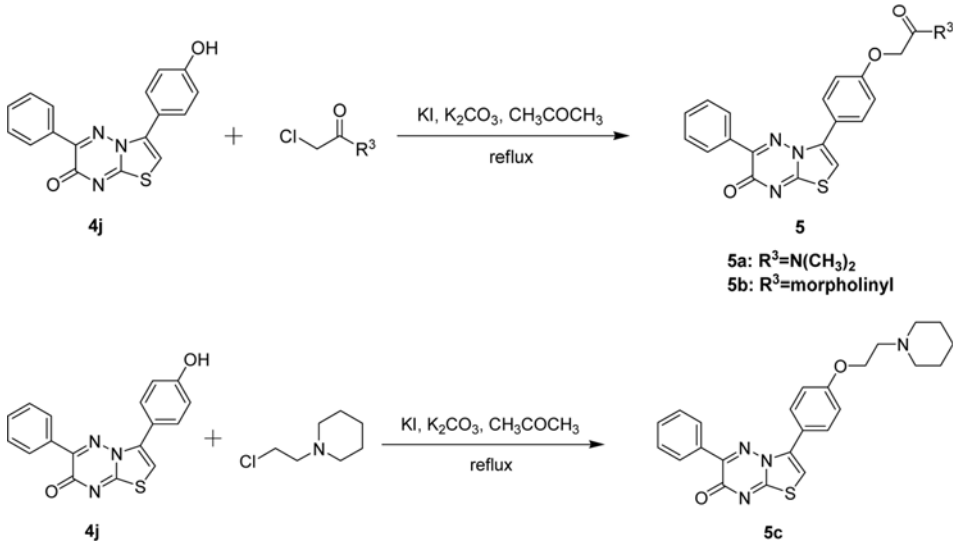

Scheme 2. The synthetic route of 3-substituted aryl 7*H*-thiazolo[3,2-*b*]-1,2,4-triazin-7-one derivatives

Table III. Inhibition of AChE activity by the target compounds

No.	Inhibition (%)	No.	Inhibition (%)	No.	Inhibition (%)
4a	38.49	**4f**	68.18	**4k**	74.75
4b	51.90	**4g**	75.30	**5a**	68.45
4c	51.06	**4h**	70.45	**5b**	63.92
4d	49.43	**4i**	82.48	**5c**	60.13
4e	65.51	**4j**	61.27		

The biological activity of *h*AChE (0.5 units) was tested against the target compounds. Each compound was tested three times (n=3), while shaking for 20 min. Inhibition of *h*AChE activity by the positive control, huperzine-A, (10 μM; n=3) was 100%.

(Fig. 2). The compounds **5a-c**, which have long side chains at the phenyl ring at the C3 position of the parent nucleus, were more potent than **4a-d** because the long side chains of **5a-c** were able to form a hydrogen bond with Ser203 located in the CAS of the AChE receptor (Fig. 3). **4f-i** and **4k** also had a strong inhibitory effect, possibly due to the halogen atoms.

Molecular force field analysis

The Field Templater software and the Field Align software were used for analyzing the molecular force fields of the target compounds. The field point template was built from compounds **4g**, **4h**, **4i**, **4k**, and **5a** using the Field Templater (Fig. 4). These five target compounds showed a stronger inhibitory activity against AChE than the other compounds. Different color balls indicated the field points, which were color coded as follows: negative ionic fields are shown in blue, positive ionic fields are shown in red, van der Waal's surface is shown in yellow, and hydrophobic fields are shown in orange. The size of the points indicates the potential strength of the interactions; the large points indicate a strong interaction. As shown by the field point patterns (Fig. 5), some target compounds, of which the inhibitory activities against

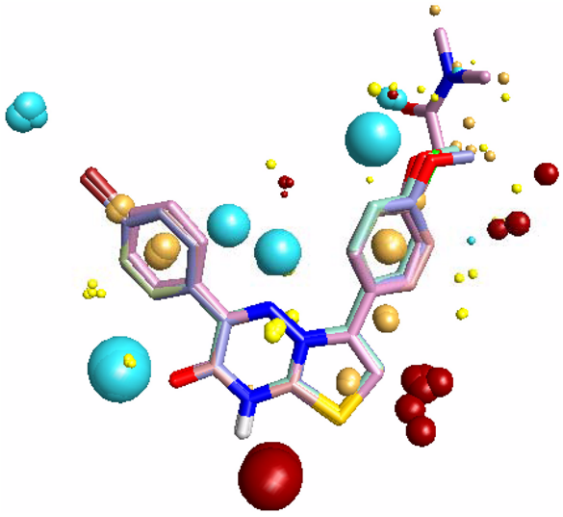

Fig. 4. Field point template of compounds **4g**, **4h**, **4i**, **4k**, and **5a**

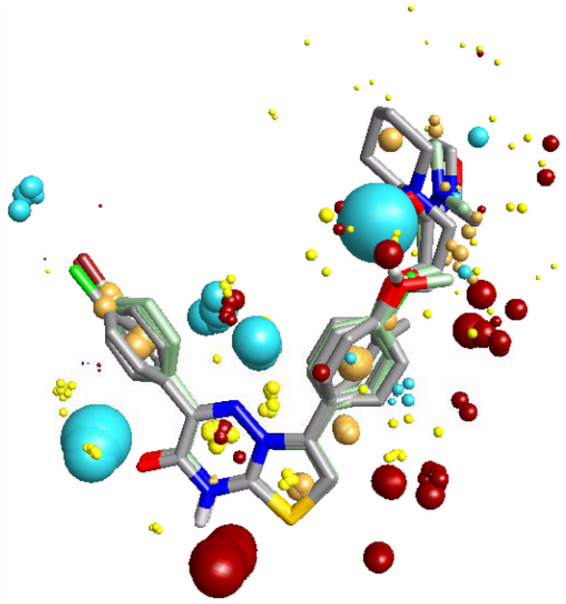

Fig. 5. Field point patterns of some target compounds

AChE were above 60%, aligned onto the template which was built in Fig. 4. The negative ionic fields are mainly located at the C8 position, and the long side chains at the phenyl ring at C3 position of the parent nucleus, as well as the para-position of the phenyl ring at C6 position of the parent nucleus. The positive ionic fields are mainly located at the C7 position. The phenyl rings form hydrophobic fields.

These phenomena showed that the CAS, the PAS and the anionic binding site are the main active sites of 3,6-diaryl-7*H*-thiazolo-[3,2-*b*][1,2,4]triazin-7-one derivatives. The hydroxyl groups, the halogen atoms, the long side chains at the phenyl ring at the C3 position, and the halogen atoms at the C6 position of the parent nucleus played significant roles in AChE inhibitory activity.

ACKNOWLEDGEMENTS

This work was supported by the National Science Foundation of China (NFSC) for the grant No. 21072130. The authors would like to thank Molegro ApS and Cresset BioMolecular Discovery Ltd. for kindly providing us with a free evaluation of their software packages. The authors would also like to thank Ms. He Zhu from Shandong University for acquiring the NMR spectra data.

REFERENCES

Ahmad, R., Hasan, A., and Ajaz, S., Synthesis & antimicrobial activity of 6-benzyl/p-substitutedbenzyl-1,2,4-triazine-3,5-(2*H*,4*H*)-dithione. *Indian J. Chem.*, 26B, 393-394 (1987).

Bai, D. L., Tang, X. C., and He, X. C., Huperzine A, a potential therapeutic agent for treatment of Alzheimer's disease. *Curr. Med. Chem.*, 7, 355-374 (2000).

Ceballos, M. L. and Guzman, M., The role of cannabinoids in preventing the neurodegenerative process occurring in Alzheimer's disease. *Drugs Future*, 30, 807-814 (2005).

Davis, K. L. and Powchik, P., Tacrine. *Lancet*, 345, 625-630 (1995).

Elsinghorst, P. W., Tanarro, C. M., and Gutschow, M., Novel heterobivalent tacrine derivatives as cholinesterase inhibitors with notable selectivity toward butyrylcholinesterase. *J. Med. Chem.*, 49, 7540-7544 (2006).

Grossberg, G. T., Effect of rivastigmine in the treatment of behavioral disturbances associated with dementia: review of neuropsychiatric impairment in Alzheimer's disease. *Curr. Med. Res. Opin.*, 21, 1631-1639 (2005).

Hebert, L. E., Scherr, P. A., and Bienias, J. L., Alzheimer disease in the US population: prevalence estimates using 2000 census. *Arch. Neurol.*, 60, 1119-1122 (2003).

Inestrosa, N. C., Alvarez, A., Perez, C. A., Moreno, R. D., Vicente, M., Linker, C., Casanueva, O. I., Soto, C., and Garrido, J., Acetylcholinesterase accelerates assembly of amyloid-beta-peptides into Alzheimer's fibrils: possible role of the peripheral site of the enzyme. *Neuron*, 16, 881-891 (1996).

Khalid, A., Zaheer-ul-Haq, Anjum. S., Khan, M. R., Atta-ur-Rahman, and Choudhay, M. I., Kinetics and structure-activity relationship studies on pregnane-type steroidal alkaloids that inhibit cholinesterases. *Bioorg. Med. Chem.*, 12, 1995-2003 (2004).

Kryger, G., Silman, I., and Sussman, J. L., Structure of acetylcholinesterase complexed with E-2020: implications for the design of new anti-Alzheimer drugs. *Structure*, 7, 297-307 (1999).

LaFerla, F. M., Green, K. N., and Oddo, S., Intracellular amyloid-beta in Alzheimer's disease. *Nat. Rev. Neurosci.*, 8, 499-509 (2007).

Liu, K. C., Shih, B. J., and Lee, C. H., Cyclocondensation of 3-amino-2-iminonaphtho[1,2-*d*] thiazole with α-ketocarboxylic acid derivatives: synthesis of 2-substituted 3-oxo-3*H*-naphtho [1',2':4,5]thiazolo[3,2-*b*][1,2,4]triazines as potential anti-HIV agents. *J. Heterocycl. Chem.*, 29, 97-101 (1992).

Liu, S. J., Yang, L., Jin, Z., Huang, E. F., Wan, D. D., Lin, H. Q., and Hu, C., Design, synthesis, and biological evaluation of 7*H*-thiazolo[3,2-*b*]-1,2,4-triazin-7-one derivatives as a novel acetylcholinesterase inhibitors. *ARKIVOC*, x, 333-348 (2009).

Marvel, C. S. and Schertz, G. L., Copolymers of p-chlorostyrene and methyl methacrylate. *J. Am. Chem. Soc.*, 65, 2054-2058 (1943).

Polinsky, R. J., Clinical pharmacology of rivastigmine: a new-generation acetylcholinesterase inhibitor for the treatment of Alzheimer's disease. *Clin. Ther.*, 20, 634-647 (1998).

Ramadan, E. S., Hamid, H. A., and Hagar, M., Synthesis of azlactones, phenylpyruvic acid and 1,2,4-triazine derivatives under microwave irradiation. *Lett. Org. Chem.*, 2, 415-418 (2005).

Raves, M. L., Harel, M., Pang, Y. P., Silman, I., Kozikowski, A. P., and Sussman, J. L., Structure of acetylcholinesterase complexed with the nootropic alkaloid, (-)-huperzine A. *Nat. Struct. Biol.*, 4, 57-63 (1997).

Reyes, A. E., Perez, D. R., Alvarez, A., Garrido, J., Gentry, M. K., Doctor, B. P., and Inestrosa, N. C., A monoclonal antibody against acetylcholinesterase inhibits the formation of amyloid fibrils induced by the enzyme. *Biochem. Biophys. Res. Commun.*, 232, 652-655 (1997).

Shao, D. and Li, Y. C., Studies on structure-activity relationships of acetylcholinesterase inhibitors. *Prog. Pharm. Sci.*, 28, 433-437 (2004).

Sussman, J. L., Harel, M., Frolow, F., Oefner, C., Goldman, A., Toker, L., and Silman, I., Atomic structure of acetylcholinesterase from *Torpedo californica*: a prototypic acetylcholine-binding protein. *Science*, 253, 872-879 (1991).

Thomsen, R. and Christensen, M. H., MolDock: A new technique for high-accuracy molecular docking. *J. Med. Chem.*, 49, 3315-3321 (2006).

Tsuno, N., Donepezil in the treatment of patients with Alzheimer's disease. *Expert Rev. Neurother.*, 9, 591-598 (2009).

Wang, L. H., Tong, R. J., Qian, Z. P., and Zhu, M. Q., Analysis and comparison of the drugs utilization for senile dementia in the past 3 years in Shanghai and Huadong Hospital. *Pharm. Care Res.*, 2, 287-292 (2002).

Zhi, H., Chen, L. M., Zhang, L. L., Liu, S. J., Wan, D. D., Lin, H. Q., and Hu, C., Design, synthesis, and biological evaluation of 5*H*-thiazolo[3,2-a]pyrimidine derivatives as a new type of acetylcholinesterase inhibitors. *ARKIVOC*, xiii, 266-277 (2008).